



Low sensitivity of a heavily-calcified coccolithophore under increasing CO₂: the case study of *Helicosphaera carteri*

Stefania Bianco^{†1,2}, Manuela Bordiga^{†3}, Gerald Langer^{*4}, Patrizia Ziveri^{4,5}, Federica Cerino³, Andrea S. Di Giulio², Claudia Lupi²

5 ¹University School for Advanced Studies IUSS of Pavia, Pavia, 27100, Italy

²Department of Earth and Environmental Sciences, University of Pavia, Pavia, 27100, Italy

³National Institute of Oceanography and Applied Geophysics - OGS, Trieste, 34151, Italy

⁴Institute of Environmental Science and Technology, Universitat Autònoma de Barcelona (ICTA-UAB), Barcelona, 08193, Spain

10 ⁵Catalan Institution for Research and Advanced Studies (ICREA), Barcelona, 08010, Spain

†These authors contributed equally to this work

Correspondence to: Gerald Langer (Gerald.Langer@uab.cat)

Abstract. Studies on CO₂ effects on coccolithophores, unicellular calcifying phytoplankton, show species-specific
15 responses, although only less than 5% of the ~280 living species have been tested so far. *Helicosphaera carteri* significantly
contributes to carbon fluxes and CaCO₃ storage due to its size and high calcite production. Despite its importance, few
studies have examined *H. carteri* under experimental conditions, and only one has addressed the effects of rising
CO₂/decreasing pH. Being *H. carteri* a large-sized, obligated calcifier species, an important aspect to understand is how
20 changes in seawater carbonate chemistry may affect its morphology. It has already been suggested for other
coccolithophores species, that the presence of malformed coccoliths may represent a disadvantage for these organisms.
Moreover, an alteration in coccolith morphology may affect their contribution to CaCO₃ sedimentation and ballasting. As for
H. carteri, it has also been suggested that due to its high PIC:POC ratio, the species could show a high-sensitivity to CO₂
rise. In this study, we investigate for the first time whether high pCO₂/low pH does affect the morphology of *H. carteri*
coccoliths, by culturing this species under pre-industrial CO₂ levels (~295 µatm) and ~600 µatm, i.e., the SSP 2-4.5 scenario
25 for 2100 (IPCC, 2021). We also analyzed cellular PIC and POC quotas using morphometric data, roundness, and protoplast
and coccosphere size to observe the pCO₂ influence on the calcification and photosynthesis ratio.

Our results indicate that *H. carteri* morphology is only slightly affected by increasing CO₂, in contrast to other heavily
calcified species. *Helicosphaera carteri* protoplast and coccosphere shapes did not vary with changes in CO₂, indicating
unaltered general health. The low PIC:POC ratio found in this work for *H. carteri* compared to ratios previously measured in
30 the same strain under different experimental conditions, and compared to other highly-calcified species, could explain the
observed low sensitivity of *H. carteri* to CO₂. Moreover, the observation of a stable ratio between calcification and
photosynthesis in *H. carteri* under increasing CO₂ might suggest a constant contribution to the rain ratio under climate



change. However, further studies comparing experimental and field data from past ocean acidification events will be required to confirm the conclusions drawn here.

35 1 Introduction

Since the industrial revolution, human activities have led to a rapid increase in atmospheric CO₂ concentration. A large amount of this emitted CO₂ (~30%) is absorbed by the oceans (Canadell et al., 2007; Sabine et al., 2004), causing a significant imbalance in the ocean chemistry, which is moving more and more towards lower pH values (IPCC, 2021).

To date, several studies have focused on the effects of seawater carbonate chemistry on calcifying organisms, including coccolithophores (e.g., D'Amario et al., 2020; Dong et al., 2023; Gattuso et al., 1998; Gazeau et al., 2024; Jokiel et al., 2008; Keul et al., 2013; Langdon et al., 2000; Riebesell et al., 2000; Ries et al., 2011), and different and sometimes contrasting evidence have been collected for this group (e.g., Iglesias-Rodriguez et al., 2008; Kroeker et al., 2013; Langer et al., 2006; Meyer & Riebesell, 2015; Raven & Crawford, 2012; Riebesell et al., 2000). Up to now, these studies have also demonstrated that to predict the responses of this group of calcifying microalgae, the consideration of different species is required. Indeed, while at the beginning, most of the efforts have been focused on common and easy-to-grow species, such as *Emiliania huxleyi* and *Gephyrocapsa oceanica*, in the last two decades, many studies have also focused on other species, like *Calcidiscus leptoporus*, *Calcidiscus quadriperforatus*, *Coccolithus pelagicus* subsp. *braarudii* and *Scyphosphaera apsteinii* (e.g., Diner et al., 2015; Fiorini et al., 2011; Gafar et al., 2019a, b; Krug et al., 2011; Langer et al., 2006; Langer and Bode, 2011). The latter species are characterized by lower abundances compared to *E. huxleyi*, but nevertheless play an important role in coccolithophore CaCO₃ production in modern oceans (Baumann et al., 2004; Daniels et al., 2014, 2016; Gafar et al., 2019b; Menschel et al., 2016; Ziveri et al., 2007).

Another low-abundant but highly contributing to CaCO₃ production is *Helicosphaera carteri* that is considered one of the main contributors to carbon (C) export and storage into deep-sea sediments (Ziveri et al., 2007), thanks to its large size and higher rates of organic C fixation and calcite production, compared to smaller species (García-Romero et al., 2017; Menschel et al., 2016; Rigual Hernández et al., 2020; Young & Ziveri, 2000). Indeed, while *E. huxleyi* produces between ~6 and ~20 pg cell⁻¹ day⁻¹ of calcite, *H. carteri* produces more than 100 pg C cell⁻¹ day⁻¹ (De Bodt et al., 2010; Langer et al., 2009; Šupraha et al., 2015).

Despite its relevant role, only a few studies have been conducted on living *H. carteri* under experimental conditions (e.g., Sheward et al., 2017; Šupraha et al., 2015; Šupraha & Henderiks 2020) and only one of them took into account the effects of CO₂ increase on this species (Le Guevel et al., 2024). To assess the potential effects of CO₂ increasing/pH lowering on coccolithophores, it is fundamental to study not only changes in calcite production, but also in coccolith morphology, as previously suggested by Langer et al. (2011). Indeed, despite the coccosphere's function is still unclear and might differ among species (Monteiro et al., 2016), studies on coccolithogenesis and coccolith structure and morphology have suggested that these calcite plates represent an advantage, and in some cases a necessity, for coccolithophores (e.g., Henriksen et al.,



65 2003; Langer et al., 2021; Walker et al., 2018). Coccoliths morphology represents a key factor in their ecology (Bown et al.,
2004; Young, 1994) and the inhibition or alteration of coccolithophores' ability to calcify can be detrimental for most of the
species belonging to this group, as demonstrated by Walker et al. (2018) for *C. braarudii*. Previous studies have also shown
that increasing CO₂/decreasing pH can strongly affect coccolithogenesis and coccolith morphology, especially when
70 considering species bearing big-sized and heavily-calcified coccoliths, with a possible detrimental influence on the ability of
these organisms to face future climate changes (Diner et al., 2015; Kottmeier et al., 2022; Langer et al., 2006; Langer and
Bode 2011).

Given the importance of *H. carteri*'s role in the C cycle, we investigate here for the first time whether rising pCO₂ does
affect coccolith morphology in this species by analyzing the presence of malformations in *H. carteri* cultures grown under
pre-industrial CO₂ levels (~290 µatm) and ~600 µatm i.e., scenario SSP 2-4.5 for 2100 (IPCC, 2021). Additionally, we
75 analyze variations in cellular particulate organic (POC), and inorganic (PIC) carbon using morphometric data (e.g.,
protoplast size, number of coccoliths per coccosphere, coccolith length) and investigate the variations in protoplast and
coccosphere size and roundness (RD).

2 Materials and methods

2.1 Experimental setting and chemical analyses

80 Monospecific cultures of *Helicosphaera carteri* (strain RCC1323, from Roscoff Culture Collection) were grown in natural
sterile-filtered seawater collected in the Gulf of Trieste (northern Adriatic Sea, Italy), filtered through 0.22 µm pore size
Durapore membrane filters (Millipore) and autoclaved, and enriched with vitamins, nutrients, and trace elements following
the B medium recipe (<https://cosmi.ogs.it/node/7>). Culture experiments were performed at the National Institute of
Oceanography and Applied Geophysics (OGS) in Trieste using the dilute batch culture method (Langer et al., 2013) and
85 keeping constant salinity (35 PSU), temperature (19°C), light irradiance (100 µmol m⁻² s⁻¹), light/dark cycle (12:12 hours)
under two different levels of CO₂ (295 and 600 µatm) in 2.5L photobioreactors (Kbiotech) controlled by the BioFlex
software. A pitched-blade impeller at 100 rpm rotational speed ensured the culture agitation. Before starting the experiments
at different CO₂ levels, the strain was acclimated for ca. 11 generations to the selected CO₂ concentration. Both experiments
were run in triplicate. All the experiments were terminated in the exponential phase at low cell density (ca. 10,000 cell mL⁻¹),
90 i.e., in dilute batch mode, corresponding to 6 or 7 days from the inoculation.

To calculate the pH values corresponding to the two selected carbon dioxide concentrations, Total Alkalinity (TA) was
measured before starting the experiments. Then, inserting TA, temperature, salinity, phosphate, and silicate data in the
CO2SYS program (Lewis and Wallace, 1998), using the constants of Mehrbach et al. (1973) refitted by Dickson and Millero
(1987), we identified a pH of 8.18 for 295 µatm, and 7.81 for 600 µatm. The pH was maintained constant for the entire
95 duration of the experiments by CO₂ injection into the headspace or by adding NaOH (1M) in the culture through an



automated peristaltic pump controlled by the BioFlex software. The pH was measured with a sensor (Hamilton PHI 225; sensitivity 57-59 mV; frequency of measurements 10 seconds) inserted within the photobioreactor.

To better characterize the carbonate system and the equilibrium among the parameters involved, Dissolved Inorganic Carbon (DIC) and Total Alkalinity (TA) were measured in two replicas on the final day of the experiment as follows.

100 For DIC analysis, the culture was filtered through pre-combusted 0.7 μm nominal pore size glass fiber filters (Whatman GF/F), and two samples of 50 mL were collected minimizing gas exchange with the atmosphere, and then poisoned with mercuric chloride (HgCl_2) solution in order to prevent biological activity. Samples were stored refrigerated until analyzed. DIC was determined using the Shimadzu TOC-V CSH analyzer. For DIC, samples were injected into the instrument port and directly acidified with phosphoric acid (25%). Phosphoric acidification for DIC and combustion conducted at 680°C,
105 generated CO_2 that was carried to a non-dispersive infrared detector (NDIR). The variation coefficient of the analyses was <2%; and the reproducibility of the method ranged between 1.5 and 3%.

For the TA, 100 mL of culture were filtered through pre-combusted 0.7 μm nominal pore size glass fiber filters (Whatman GF/F), poisoned with 100 μL of saturated mercuric chloride (HgCl_2) to halt the biological activity, and stored in acid-washed borosilicate flasks at 4°C. TA was measured by potentiometric titration in an open cell (SOP 3b, Dickson et al., 2007)
110 utilizing a non-linear least squares approach. The titration was conducted with the Mettler Toledo G20 titration unit interfaced with a computer, using the LabX data-acquisition software. After titration, data were processed and the TA was calculated using a computer program developed at OGS and adapted to work in association with the Mettler Toledo LabX software and similar to that listed in SOP 3 of DOE (Dickson and Goyet, 1994). The HCl titrant solution (0.1 mol kg^{-1}) was prepared in NaCl background, to approximate the ionic strength of the samples, and was calibrated using certified reference
115 seawater (CRM, Batch #107, provided by A.G. Dickson, Scripps Institution of Oceanography, USA). Accuracy and precision of the TA measurements on CRM were determined to be less than $\pm 2.0 \mu\text{mol kg}^{-1}$.

The final carbonate system was calculated from temperature, salinity, TA, pH (NBS), phosphate and silicate, using the CO2SYS program (Lewis and Wallace, 1998), with the same constants mentioned above. The data for the carbonate system are reported in Table 1.

120

Parameter	Exp. 295	Exp. 600
CO_2 (μatm)	294.6	601.5
CO_2 ($\mu\text{mol/kg}$)	9.78	19.94
HCO_3^- ($\mu\text{mol/kg}$)	1413.49	1213.70
CO_3^{2-} ($\mu\text{mol/kg}$)	141.44	51.72



DIC ($\mu\text{mol/kg}$)	1677.50	1374.72
TA (mmol/kg^{-1})	1853.82	1452.54
pH NBS	8.18	7.81
Ω calcite	3.38	1.24

Table 1. Parameters of the carbonate system. In black are the values obtained from the CO2SYS program; in blue are the average values directly measured in duplicates per each replica of both the experiments. The average pH values are derived from the whole data collected in continuum along the experiments (pH standard deviation 0.01).

125 2.2 Morphological analyses

Helicosphaera carteri coccospheres were collected from triplicate cultures and filtered on cellulose acetate filters (Ø 25 mm pore Ø 0.45 μm) for subsequent analyses at the Scanning Electron Microscope (SEM). Filters were dried at 30°C for 24 hours. The filters were mounted using carbon tapes on SEM stubs, and then sputter-coated with gold-palladium using the Emitech K550X/K250 C cathodic metallizer. Analyses at SEM were conducted with a Zeiss Merlin at the Microscopy and

130 X-ray Diffraction Service of the Universitat Autònoma de Barcelona.

After a preliminary observation of the samples, we subdivided the morphologies of *H. carteri* coccoliths in two main categories: normal and malformed (Fig. 1). At the SEM we observed that the malformations occurring in *H. carteri* coccoliths are often characterized by underdevelopment or abnormal development of the flange (Fig. 1c, d). Sometimes, the malformation is also represented by coccoliths presenting a "wavy" shape (Fig. 1c, d). Per sample at least 100 coccoliths

135 were counted, for a total of ~300 coccoliths per experiment (Table 2).

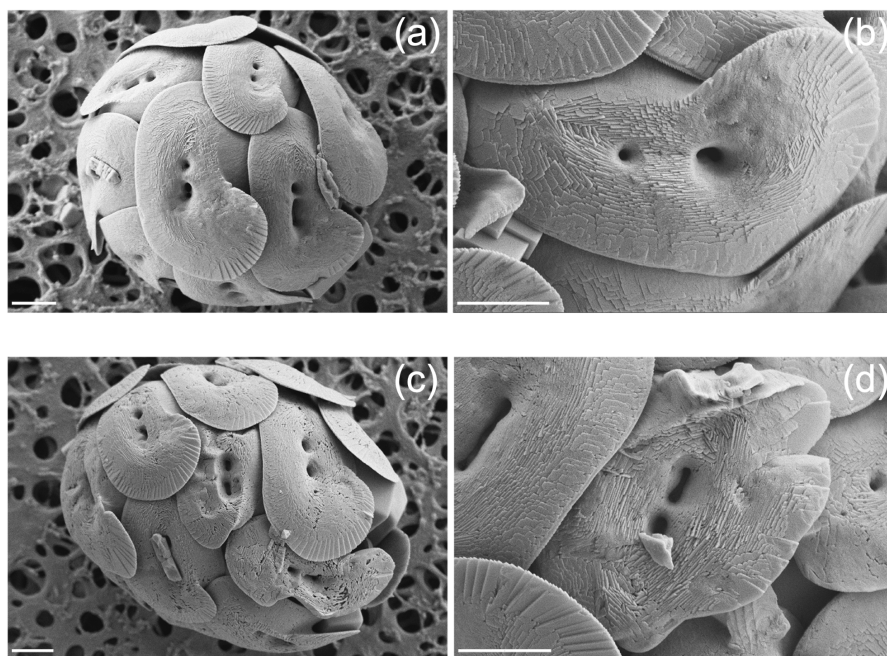


Figure 1. Scanning electron micrographs of *Helicosphaera carteri* coccoliths. (a, b) normal (c, d) malformed. Scale bars are 2 μm .

140 2.3 Morphometric analyses

2.3.1 Cocosphere measurements and PIC calculation

On the last day of each experiment, 1mL of culture was collected and combined with 4 μL of Formalin for cocosphere morphometric analysis. Cocosphere size (\emptyset), aspect ratio ($AR_{\text{cocosphere}}$) and roundness ($RD_{\text{cocosphere}}$) data were obtained by photographing more than 50 cocospheres per each replicate using an inverted microscope Leica CMS-D35578 and a Leica
 145 Camera Ltd CH-9435. The images were processed with ImageJ software (Rueden et al., 2017; Appendix A Fig. A1) using a customized macro (<https://github.com/mbordiga/Coccoliths>). $AR_{\text{cocosphere}}$ and $RD_{\text{cocosphere}}$ were strongly correlated (-0.99, p-value <0.0001); therefore, only RD data have been discussed in this work. RD values closer to 1 indicate a more circular shape (for details see Appendix A Table A1).

The cellular particulate inorganic carbon (cellular PIC) of *H. carteri* was estimated from cocosphere geometry data,
 150 following Young and Ziveri (2000):

$$\frac{PIC[p\text{g}]}{cell} = C_N \times C_L^3 \times K_s \times \rho \times \left(\frac{M_C}{M_{CaCO_3}} \right), \quad (1)$$



Where C_N is the number of coccoliths per coccosphere, C_L^3 is the coccolith length (μm), k_s is the mean species-specific
155 dimensionless shape factor (0.05 for *H. carteri*; Young and Ziveri 2000), ρ is the calcite density ($2.7 \text{ pg } \mu\text{m}^3$) and $\frac{M_C}{M_{\text{CaCO}_3}}$ is
the molar mass ratio of C and CaCO_3 (0.12).

The number of coccoliths per cell (C_N) was determined from the samples previously used for counting malformed coccoliths
(see Sect. 2.2). At least 50 photographs of coccospheres were captured using the SEM and the number of coccoliths per cell
was estimated by visually counting the visible ones and assuming they represent 75% of the total (as demonstrated for *E.*
160 *huxleyi* in Hoffmann et al., 2015).

The averages data used for the calculation and the number of individuals analyzed are reported in the Appendix (Appendix A
Table A1).

For single coccolith measurements, additional culture samples were obtained by treating 25 mL of culture with 25 mL of a
Triton (1%) and 20 microL bleach solution to separate them from the cell (see Šupraha & Henderiks, 2020).

165 Part of the obtained pellet was then added to a solution of distilled water buffer with ammonia (1L distilled water + 30 mL of
25% ammonia solution). A small amount of this suspension was subsequently pipetted onto a round glass coverslip (\emptyset 13
mm) and dried on a hot plate at 60°C . The coverslip was then mounted on SEM stubs (\emptyset 25 mm) using a carbon disc. To
increase the sample's conductivity, four aluminum bridges connecting the coverslip to the edge of the stubs were added in
each sample. The samples were then sputter-coated with platinum and analyzed using the Tescan Mira3XMU SEM of the
170 Department of Earth and environmental Sciences at the University of Pavia (CISRIC-Arvedi Laboratory). Unfortunately, due
to an alteration in the preservation state of the material, it was not possible to analyze the third replicate of both experiments.
For the remaining samples, at least 100 coccoliths were photographed and measured using ImageJ software (Rueden et al.,
2017) for a total of 409 coccoliths (Appendix A Table A1).

Statistical analyses (unpaired t-tests) have been performed for \emptyset and $\text{RD}_{\text{coccosphere}}$ using GraphPad Prism (version 9.05 for
175 MacOS; GraphPad Software, Inc., USA).

2.3.2 Protoplast measurements and POC calculation

Helicosphaera carteri cellular POC was estimated from protoplast size, following Menden-Deuer and Lessard (2000):

$$180 \frac{\text{POC} [\text{pg}]}{\text{cell}} = a \times V_{\text{cell}}^b, \quad (2)$$

Where V_{cell}^b is the protoplast volume, and a and b are constants depending on the considered species (in this case: $a=0.216$
and $b=0.939$; Menden-Deuer and Lessard, 2000). Protoplast volume in μm was calculated as $V_{\text{cell}} = (\pi/6)d^2h$, where d and
 h represent the short and the long-axes cell diameters in μm (Sun and Liu, 2003).



185

The V_{cell} was obtained by measuring cells from culture samples collected at the T_{final} of each experiment. 4 mL of culture samples were fixed with acidic Lugol solution (40 μ L) which dissolves the coccoliths while preserving the protoplast for subsequent measurements. Protoplast size (Θ) data were obtained by analyzing at least 50 photos (collected at the inverted microscope) per sample, with ImageJ software (Rueden et al., 2017) using a custom-made macro (https://github.com/mbordiga/Coccoliths; Supplementary materials).

190

With the same macro, data about protoplast aspect ratio ($AR_{protoplast}$) and roundness ($RD_{protoplast}$), were obtained. As for the coccosphere, due to the high correlation between RD and AR, only data about cellular roundness were reported in this work. The averages of the data used for the calculation and the number of individuals analyzed are provided in the Appendix (Appendix A Table A1).

195

Changes in Θ and $RD_{protoplast}$ have been compared using an unpaired t-test on GraphPad Prism (version 9.05 for MacOS; GraphPad Software, Inc., USA).

3 Results

3.1 Coccolith morphology

200

The analyses at the SEM revealed a slight change in the proportion of malformed coccoliths moving from \sim 295 to 600 μ atm of CO_2 . Indeed, while at the lower pCO_2 , the species shows almost no malformations (0.66%), an increase in the percentage of malformed coccoliths is observed in the second treatment, where the normal coccoliths account for an average of 89.35 % (Table 2, Fig. 2). The percentage (10.65%) of malformed coccoliths at 600 μ atm is characterized by a high standard deviation (SD), suggesting a relatively high variability among the triplicates. On the contrary, at 295 μ atm, SD is quite low in all the considered categories, reflecting a greater degree of consistency between the samples compared to 600 μ atm (Table 2). None of the observed samples showed extremely malformed coccoliths. All coccospheres were intact. A rough estimation of the number of collapsed coccospheres per sample indicated a percentage far below 1%. Therefore, a specific count for this category was not performed, because it is not meaningful.

205

The saturation state of seawater with respect to calcite ($\Omega_{calcite}$), is lower at 600 μ atm than at pre-industrial CO_2 levels. However, the values are always >1 , indicating that the system is never undersaturated, indeed no dissolution has been detected (Table 1).

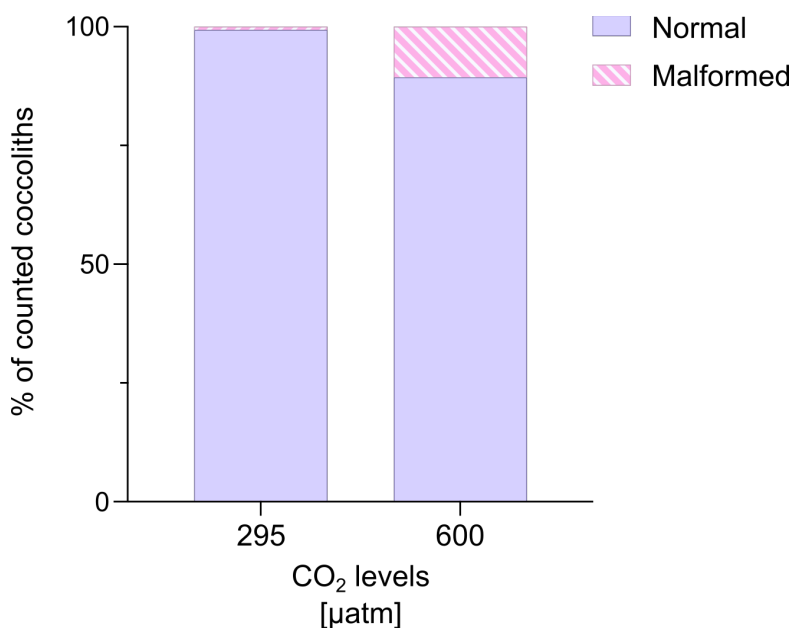
210

Experiment	CO_2 [μ atm]	Normal	Malformed	Total nr. of counted coccoliths
1	295	99.34	0.66	304



SD		2.08	0.58	
2	600	89.35	10.65	316
SD		13.87	10.82	

Table 2. Percentages of counted coccoliths at the two different CO₂ concentrations. Data reported are averages of three replicates. SD = standard deviation.



215

Figure 2. Percentages (%) of normal and malformed coccoliths of *H. carteri*. Values reported represent the averages of the three replicates.

3.2 Coccosphere and protoplast geometry

220 Cellular POC returns an average of 108.14 pg cell⁻¹ at 295 µatm and 118.51 pg cell⁻¹ at 600 µatm of CO₂. The unpaired t-test
 (performed in GraphPad Prism version 9.05 for MacOS; GraphPad Software, Inc., USA) indicates that the increase from the
 lowest to the highest CO₂ level is not statistically significant (Table 3). A non-significant change is also observed in cellular
 PIC, with values varying from 151.86 pg cell⁻¹ at 295 µatm to 149.47 pg cell⁻¹ in the second treatment. The PIC:POC ratio
 does not change significantly (Unpaired t-test p value = 0.2083) as well, decreasing from 1.37 at 295 µatm to 1.27 at 600
 225 µatm of CO₂ (Table 3).



Helicosphaera carteri protoplast and coccosphere roundness does not show any significant variation with increasing CO₂. While the first remained unchanged at the value of 0.9 ± 0.06 , the second decreased from 0.89 ± 0.05 to 0.88 ± 0.06 indicating the maintenance of a constant shape at different CO₂ levels (Fig. 3 a, b).

230 A non-significant change in protoplast and coccosphere size with increasing CO₂ can also be observed, with the protoplast size increasing from 11.45 to 11.81 μm and the coccosphere size decreasing from 18.18 to 17.92 μm (Fig. 3 c, d; Appendix A Table A1). The range of protoplast size does not change very much, from 295 to 600 μatm; while for the coccosphere size, a slightly higher range is recorded at the higher CO₂ level (Fig. 3 c, d; Appendix A Table A1).

CO ₂		295	600	p value
[μatm]				
PIC [pg cell ⁻¹]	Mean	151.86	149.47	0.7755
	SD	4.23	9.49	
POC [pg cell ⁻¹]	Mean	108.14	118.51	0.1000
	SD	22.54	23.71	
PIC:POC		1.37	1.27	

235 **Table 3. Data of *H. carteri* cellular PIC and POC obtained from geometry data. Values reported are averages of the replicates. SD = standard deviation.**

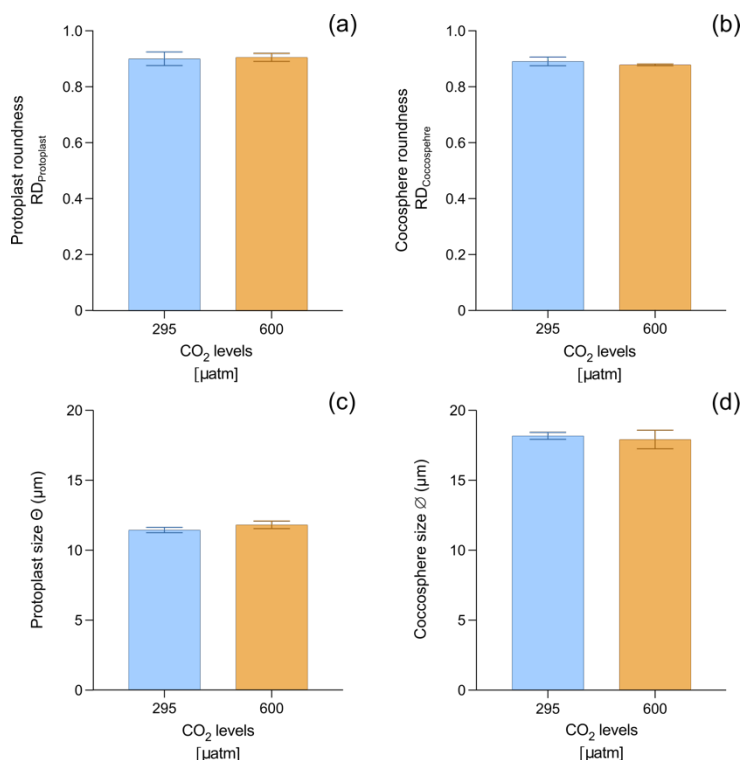


Figure 3. Data of *H. carteri* roundness and size, measured on the protoplast (a, c) and coccosphere (b, d). Reported values are averages of three replicates. Error bars show standard deviation.

4 Discussion

240 4.1 Malformations in *H. carteri* in response to CO₂ increase

In the recent years, several studies have focused on coccolithophores' responses under increasing CO₂ levels, demonstrating that different species, and often different strains of the same species, exhibit a specific at times contrasting response to seawater carbonate chemistry (e.g., Bach et al., 2015; Diner et al., 2015; Langer et al., 2006, 2009, 2011; Langer and Bode 2011). These non-uniform results have highlighted the need to analyze the CO₂ influence on both coccolithophore species and strains to better predict the whole group reaction to future climate change.

To evaluate the coccolithophore response under high CO₂, a key but sometimes neglected parameters are the degree of coccolith malformation and data on morphometrics. To date, few studies have evaluated coccolith morphology (i.e., normal, malformed, or incomplete coccoliths) under seawater carbonate chemistry changes not only in a qualitative way, but also in a quantitative way (e.g., Bach et al., 2011, 2012; De Bodt et al., 2010; Diner et al., 2015; Kottmeier et al., 2022; Langer et al., 2006, 2011), but none of them considered the species *H. carteri*. Coccolith morphology is central to ecological and evolutionary success of coccolithophores and is often more telling than calcite production when questions concern the



biology, as opposed to the biogeochemistry, of these algae (Henriksen et al., 2003; Langer et al., 2011, 2021; Walker et al., 2018).

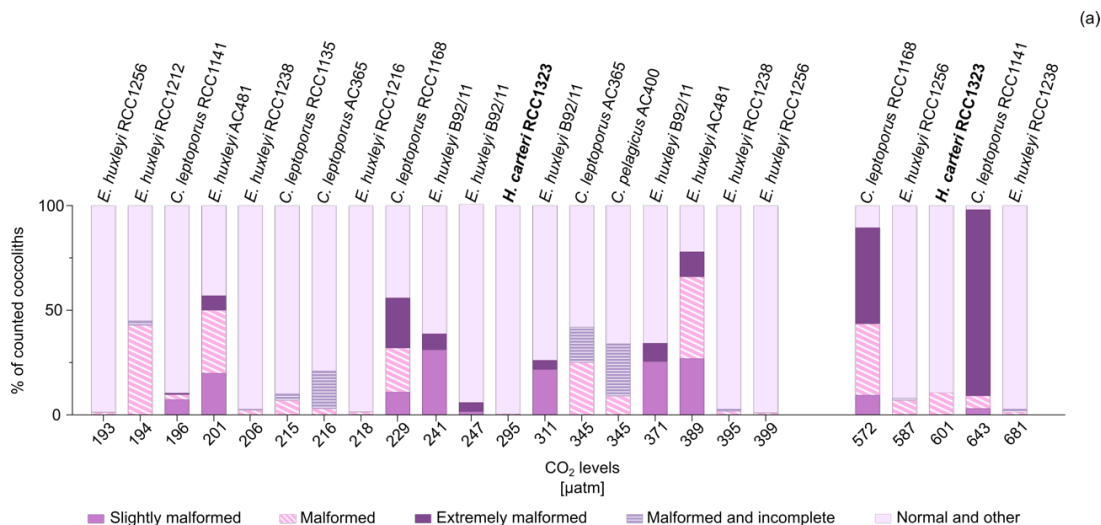
In this work, for the first time, we show that the percentage of malformed coccoliths in *H. carteri* increases from 295 to 600
255 μatm of CO_2 . However, when comparing our findings for *H. carteri* with previous works conducted on other species, it is
evident that for most species and strains the percentage of malformed coccoliths at CO_2 levels similar to 295 μatm (± 100
 μatm) is higher (Fig. 4a, b). Specifically, a greater percentage of malformed coccoliths (considering all the categories
defined by the authors) was observed in six different strains of *E. huxleyi* (RCC1238, RCC1216, RCC 1256, RCC1212,
B92/11, AC481), four strains of *C. leptoporus* (AC365, RCC1135, RCC1141, RCC1168), and one strain (AC400) of *C.*
260 *pelagicus* (Fig. 4 a, b).

When considering responses to CO_2 levels close to 600 μatm , the percentages of malformed coccoliths in *E. huxleyi*
(RCC1238 and RCC1256) are lower than *H. carteri* (Fig. 4a, c). In contrast, the heavily calcified species *C. leptoporus*
(RCC1168) and *C. quadriperforatus* (RCC1141) consistently show a higher percentage of malformed coccoliths compared
to *H. carteri* ($\sim 90\%$, Fig. 4a, c). It is interesting to note that these percentages also include a significant amount of extremely
265 malformed coccoliths (89% for *C. quadriperforatus* RCC1141, and 46% for *C. leptoporus* RCC1168; Fig. 4a). This degree
of malformation has never been observed in our experiments. Since biological parameters such as coccolith morphology
undergo numerical changes over time (Langer et al., 2013), the assessment of species sensitivity should not be based on the
morphology of different strains or species at one CO_2 level alone, but rather the change of morphology in response to a
change in CO_2 (Hoppe et al., 2011). For example, the species *E. huxleyi* strain B92/11 shows varying percentages of
270 malformations across a narrow range of CO_2 levels, illustrating this observation (Fig. 4a, b). On the other hand, at ca. 600
 μatm CO_2 *Calcidiscus* displays more malformations than at 295 μatm of CO_2 (Fig. 4c), and the reason for this is most likely
that the negative effect of carbonate chemistry is almost invisible at ca. 300 μatm CO_2 . Using the reasoning of Bach et al.
(2015), we would say that at 300 μatm of CO_2 neither substrate limitation nor proton inhibition play a significant role, and
the malformations depend on other experimental conditions.

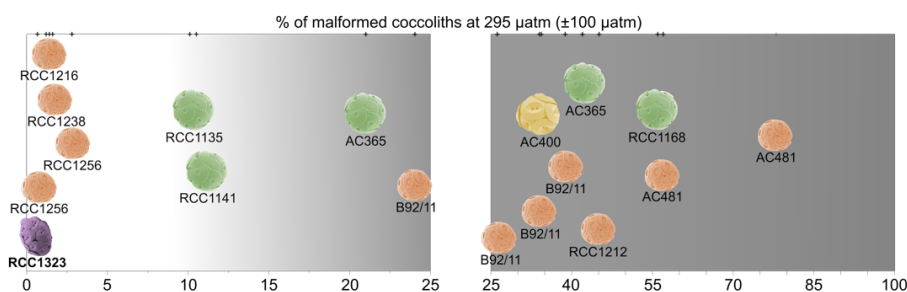
275 On the contrary, at ca. 600 μatm CO_2 the effect of proton inhibition becomes visible in *Calcidiscus* compared to *Emiliana*
and *Helicosphaera*. Therefore, the conclusion suggested by the morphology distribution in Fig. 4 is confirmed when
comparing relative changes between experiments (Fig. 4b, c; Diner et al., 2015; Hoppe et al., 2011; Langer et al., 2006,
2011; Langer and Bode, 2011). We are thus confident in saying that the strains RCC1238 and RCC1256 of *E. huxleyi* and
RCC1323 of *H. carteri* are less sensitive to acidification than *Calcidiscus*.

280 However, it is important to note that different authors have observed varying responses among different strains of both *E.*
huxleyi and *C. leptoporus*, indicating the absence of a uniform species-specific behavior, potentially linked to genotypic
diversity (see Diner et al., 2015; Langer et al., 2009). These diverse responses could be identified in *H. carteri* too.
Therefore, additional studies considering different strains of *H. carteri* will be required to identify if our evidence is strain-
specific or it can be extended to species level.

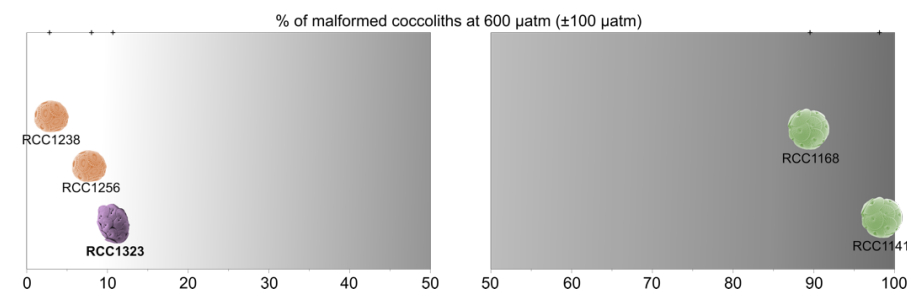
285



(a)



(b)



(c)

Figure 4. a) Percentages of malformed coccoliths in *H. carteri* (in bold; this work) compared to other species (from literature) at CO₂ levels close to 295 µatm (±100 µatm) and 600 µatm (±100 µatm). “Other” includes other categories used by the authors, such as fragmented coccoliths or incomplete coccoliths without malformations. b-c) Distribution of the considered strains according to a gradient of increasing percentage of malformation at 295 µatm (b) and 600 µatm (c). Different scales have been used. Cocosphere photos are modified from Nannotax.org. Data for comparison include *E. huxleyi* RCC1216, RCC1238, RCC1256 and RCC1212 from Langer et al. (2011); *C. leptoporus* RCC1141 and *C. quadriperforatus* RCC1168 from Diner et al. (2015); *E. huxleyi* AC481 from De Bodt et al. (2010); *C. leptoporus* RCC1135 from Langer and Bode (2011); *C. leptoporus* AC365 and *C. pelagicus* AC400 from Langer et al. (2006); *E. huxleyi* B92/11 from Bach et al. (2011).

290

295



4.2 *Helicosphaera carteri* sensitivity towards CO₂ increase

Studies on coccosphere and protoplast geometry (e.g., \emptyset , C_L , C_N) of *H. carteri* strain RCC1323 have been conducted before (Le Guevel et al., 2024; Sheward et al., 2017; Šupraha et al., 2015). However, none of these studies considered the variations in protoplast or coccosphere shapes. In this study, we show for the first time the absence of any significant variation in $RD_{\text{protoplast}}$ and $RD_{\text{coccosphere}}$ with increasing CO₂ (Fig. 3a, b). These results could indicate that the species shape does not depend on CO₂ concentrations. Daily observation of the living culture under a light microscope showed in both CO₂ treatments a good health of *H. carteri*, including good motility of the cells. These observations combined with the lack of a CO₂ effect on roundness and the small effect on coccolith morphology point to a weak sensitivity of *H. carteri* to seawater acidification/CO₂ increase (Figs. 2, 3 a, b).

In our study, we also examined the variations in the protoplast and coccosphere geometry (C_N , C_L , coccosphere and protoplast size) in response to an increase in CO₂, observing no significant changes from 295 to 600 μatm (Fig. 3, Appendix A Table A1). Since *H. carteri* \emptyset , C_L and C_N did not change between our experiments, the cellular POC and PIC content and PIC:POC ratio did not show any substantial variation with increasing CO₂ (Fig. 3c, d; Table 3, Appendix A Table A1).

A non-significant variation in coccosphere size and PIC:POC ratio in the same *H. carteri* strain and at similar CO₂ levels (300 μatm and 600 μatm) has recently been observed also by Le Guevel et al. (2024) (Fig. 5). These authors grew the species to under even higher CO₂ levels, recording a decrease in coccosphere size (-1.05 μm) moving from 600 μatm to 1400 μatm of CO₂. However, this decrease in coccosphere size with increasing CO₂/decreasing pH, was not associated with a significant trend in the PIC:POC ratio (Le Guevel et al., 2024).

Similar results were documented also in the fossil record by Šupraha & Henderiks (2020), who estimated the PIC:POC ratio for the genus *Helicosphaera* over the last 15 million years (Myr) from the lateral cross-sectional aspect ratio of a coccolith (AR_L), following McClelland et al. (2016). These authors documented a stable PIC:POC ratio of this genus along with a reduction of coccolith (and coccosphere) size in response to the global decreasing trend in CO₂ (Herbert et al., 2016; Sosdian et al., 2018; Super et al., 2018; Zachos et al., 2001; Zhang et al., 2013). Šupraha & Henderiks (2020) attributed the lack of change in the ratio between calcification and photosynthesis to the obligate calcifier nature of the genus *Helicosphaera*. The obligate calcifier-nature of *Helicosphaera* represented by the maintenance of a stable PIC:POC observed both under experimental conditions; (this work, Le Guevel et al., 2024) and in the fossil record; (Šupraha & Henderiks, 2020), could represent an advantage in future oceans where the species could play a stable role in the C cycle despite changes in CO₂ concentrations. However, to confirm this hypothesis, studies on fossil material deposited during paleo-analogues of future CO₂ rise above 600 μatm are required. Reconstructing different coccolithophore species' PIC:POC ratio during past climate events is, indeed, a fundamental tool to better predict their response also to future climate changes. Unfortunately, the chances to find entirely preserved coccospheres in the fossil record is relatively low (Henderiks et al., 2008). Thus, combining culture studies on PIC:POC estimates from coccosphere, protoplast, AR, and coccolith measurements with



330 observations conducted on fossil coccoliths represents a key tool for investigating the species-specific contribution to the organic C fixation and calcite production in the fossil record, improving our knowledge on the inorganic *versus* organic C balance in the oceans.

With regard to the relationships between PIC:POC ratio and CO₂ sensitivity of different species and strains one of the most significant and consistent evidence is that coccolithophore species with a higher PIC:POC ratio should be more sensitive to increasing CO₂ compared to species with lower average PIC:POC ratio such as *E. huxleyi* (0.67), *Syracosphaera pulchra* 335 (0.19), and *Umbilicosphaera sibogae* (0.62; Gafar et al., 2019b). The low sensitivity of species with lower PIC:POC ratio, like *E. huxleyi*, is confirmed by the comparison in Figure 4b, c, where *E. huxleyi* appears more resilient in terms of malformations to increasing CO₂ levels, compared to both *H. carteri* and *C. leptoporus*. As for *H. carteri* RCC1323, the range of PIC:POC ratio considered by Gafar et al. (2019b), based on data from Šupraha et al. (2015), spans from 2.29 to 2.30, thus a relatively high ratio leading to a first inference that this strain may be highly sensitive to CO₂ increase. However, 340 recent data about *H. carteri* PIC:POC ratio documented a lower PIC:POC values for this strain (1.27-1.37 ratio this work; ~1.4-1.6 ratio Le Guevel et al., 2024) (Fig. 5). The identification of a lower PIC:POC ratio for *H. carteri* RCC1323 (average ratio 1.8) could explain our data documenting a low sensitivity of this strain to increasing CO₂, compared to *C. leptoporus* (average ratio 2.08) and *C. quadriperforatus* (average ratio 2.01) (see Sect. 4.1; Diner et al., 2015; Gafar et al., 2019b).

However, in the literature there are sometimes contrasting results on coccolithophore sensitivity towards CO₂ in relation to 345 the PIC:POC ratio. Langer et al. (2009), while testing different strains of *E. huxleyi* grown under varying seawater chemistry conditions, documented that the strain with the highest PIC:POC ratio (RCC1216; maximum PIC:POC value 1.2) exhibited the highest percentage of normal coccoliths, corresponding to a low sensitivity towards higher CO₂. The most likely explanation for these observations is that other aspects than the PIC:POC ratio influence the species' response to increased CO₂ levels. For instance, genetic factors, as suggested by Diner et al. (2015) and Langer et al. (2009), may play a significant 350 role. This once again underscores the importance of analyzing different species and strains and under varying experimental conditions.

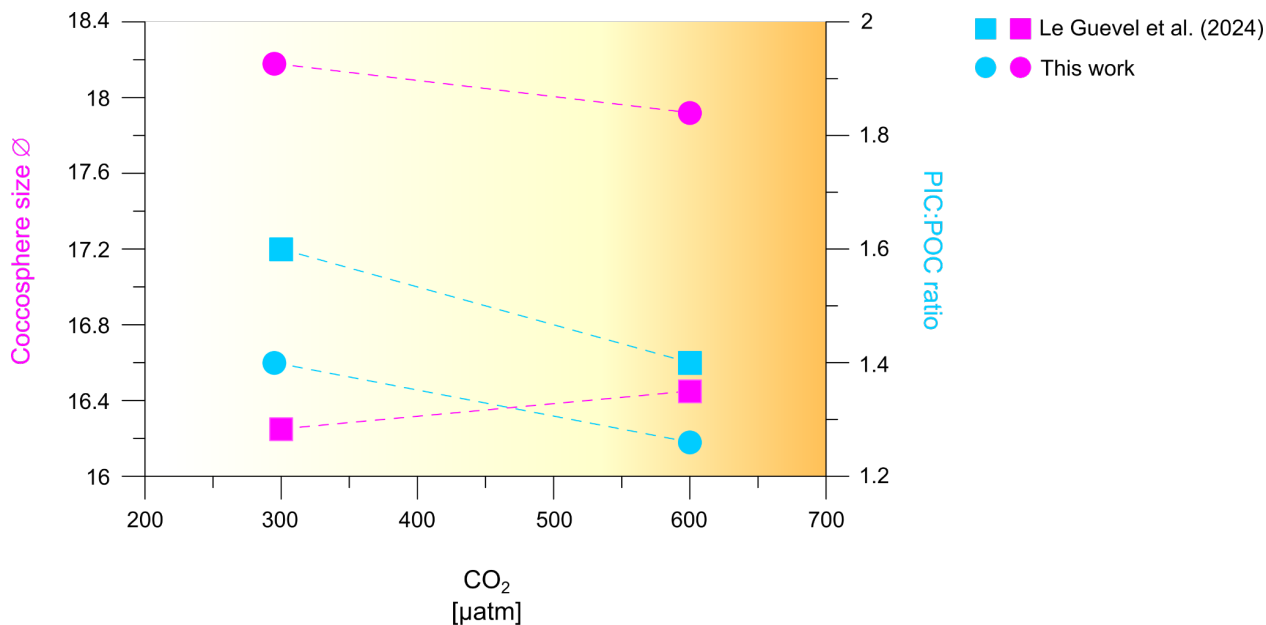


Figure 5. Comparison of coccosphere size and PIC:POC ratio of *H. carteri* under increasing CO₂, measured in this work and in Le Guevel et al. (2024).

355 5. Conclusions

Based on our findings, we can conclude that:

1. *Helicosphaera carteri*, exposed to pre-industrial CO₂ levels and 600µatm of CO₂, shows a low sensitivity to rising CO₂, as inferred from protoplast and coccosphere roundness, and chiefly from coccolith morphology.
2. The low sensitivity of *H. carteri* to high CO₂ is contrasted with the relatively high sensitivity of *Calcidiscus*. An explanation for this surprising species specificity might be the low PIC:POC of *H. carteri* determined here.
3. The PIC:POC ratio of *H. carteri* does not change with changing CO₂ suggesting a constant contribution of this species to the rain ratio under ocean acidification.

360

Appendix A: morphometric analyses

CO ₂ [µatm]		295	600
	Min	14.30	14.76
Coccosphere size Ø [µm]	Mean	18.18	17.92
	Max	21.54	23.30



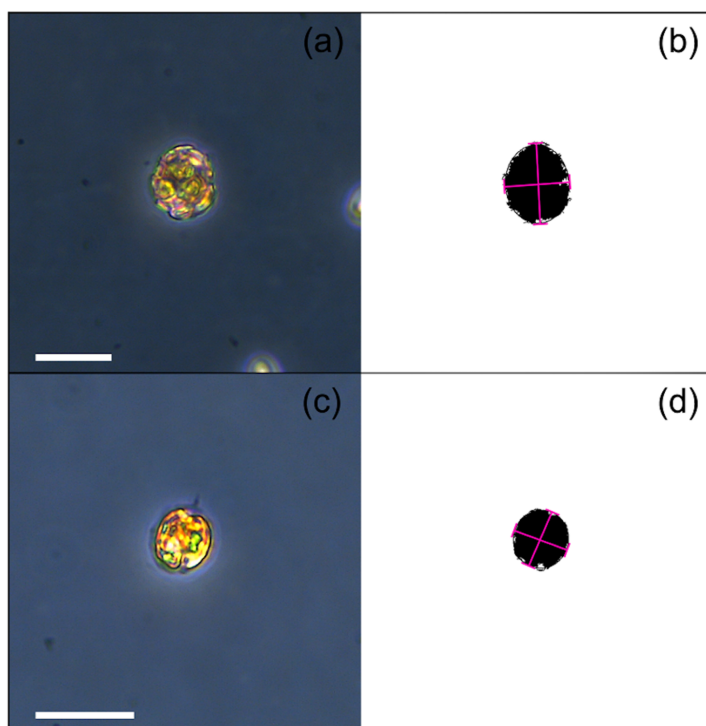
CO₂		295	600
[μatm]			
	SD	0.25	0.66
	Nr. of values	151	158
Protoplast size Θ [μm]	Min	9.59	9.74
	Mean	11.45	11.81
	Max	14.12	14.56
	SD	0.19	0.27
	Nr. of values	161	154
Coccosphere aspect ratio $AR_{coccosphere}$	Min	1.01	1.01
	Mean	1.13	1.14
	Max	1.46	1.3
	SD	0.02	0.005
	Nr. of values	151	158
Coccosphere roundness $RD_{coccosphere}$	Min	0.69	0.74
	Mean	0.89	0.88
	Max	0.99	0.99
	SD	0.02	0.003
	Nr. of values	151	158
Protoplast aspect ratio $AR_{protoplast}$	Min	1.00	1.01
	Mean	1.12	1.11
	Max	1.34	1.47
	SD	0.03	0.02
	Nr. of values	161	154
Protoplast roundness $RD_{protoplast}$	Min	0.75	0.68
	Mean	0.90	0.90
	Max	0.99	0.99
	SD	0.02	0.01
	Nr. of values	161	154



CO₂ [µatm]		295	600
Coccoliths per coccosphere C _N	Min	9	9
	Mean	15	15
	Max	20	25
	SD	0.67	0.44
	Nr. of values	167	178
Coccolith length C _L [µm]	Min	6.20	6.6
	Mean	8.65	8.60
	Max	10.01	10.33
	SD	0.07	0.04
	Nr. of values	201	207
Cellular PIC [pg cell ⁻¹]	Mean	151.86	149.47
	SD	4.23	9.50
	Nr. of values	201	207
Cellular POC [pg cell ⁻¹]	Mean	108.14	118.51
	SD	5.42	6.41
	Nr. of values	161	154

Table A1. Summary of *H. carteri* protoplast and coccosphere geometry data obtained from ImageJ Software used in this work. The values reported are the averages of the replicates. SD= standard deviation.

365



4.

Figure A1. Photo of a coccosphere (a, b) and a protoplast (c, d) before and after ImageJ processing. Measurements of the long and short axes are indicated in pink (c, d). All bars are 20 μm .

Data availability

370 The Java script used here within ImageJ Software is available on GitHub: <https://github.com/mbordiga/Coccoliths>

Author contribution

375 S.B., G.L. and M.B. conceived the study; F.C. and M.B. designed the experiments and M.B. carried out the experiments; S.B. and G.L. analyzed the coccolithophore samples, the data sets, and elaborated the data; S.B. wrote the first draft with contributions on data discussion and interpretation from G.L., M.B., and C.L.; M.B., C.L., and A.D.G. provided financial support for the project; P.Z. and A.D.G. provided a critical review. All authors contributed to the final draft.

Competing interests

The authors declare that they have no conflict of interest.



Disclaimer

380 Publisher's note: Copernicus Publications remains neutral with regard to jurisdictional claims made in the text, published maps, institutional affiliations, or any other geographical representation in this paper. While Copernicus Publications makes every effort to include appropriate place names, the final responsibility lies with the authors.

Acknowledgments

385 We thank M. P. Riccardi and M. Musa (CISRIc-Arvedi Laboratory, University of Pavia) for technical assistance during SEM analyses; M. Cabrini, A. Beran, F. Relitti, and V. A. Laudicella (OGS, Trieste) for their technical support. This work was funded by MUR for ECORD-IODP Italia 2018 to M. Bordiga within the project "Geochemistry and marine biology united to refine climate models" conducted at the National Institute of Oceanography and Applied Geophysics (OGS) and for Italian national inter-university PhD course in Sustainable Development and Climate change (link: www.phd-sdc.it) to S. Bianco. The project was also supported by C. Lupi and A. Di Giulio with University of Pavia Research Funds (FAR 2021-2023) and by the Okada-McIntyre Graduate Research Fellowship of INA awarded to S. Bianco. G. Langer acknowledges funding from the Spanish Ministry of Universities through a Maria Zambrano grant and the Generalitat de Catalunya (MERS, 2021 SGR 00640). This work contributes to ICTA-UAB "María de Maeztu" Programme for Units of Excellence of the Spanish Ministry of Science and Innovation (CEX2019-000940-M).

390

395 This paper and related research have been conducted during and with the support of the Italian national inter-university PhD course in Sustainable Development and Climate change (link: www.phd-sdc.it), and it is part of S. Bianco PhD.

References

- Bach, L. T., Riebesell, U., and Schulz, K. G.: Distinguishing between the effects of ocean acidification and ocean carbonation in the coccolithophore *Emiliana huxleyi*, *Limnology & Oceanography*, 56, 2040–2050, <https://doi.org/10.4319/lo.2011.56.6.2040>, 2011.
- 400 Bach, L. T., Bauke, C., Meier, K. J. S., Riebesell, U., and Schulz, K. G.: Influence of changing carbonate chemistry on morphology and weight of coccoliths formed by *Emiliana huxleyi*, *Biogeosciences*, 9, 3449–3463, <https://doi.org/10.5194/bg-9-3449-2012>, 2012.
- Bach, L. T., Riebesell, U., Gutowska, M. A., Federwisch, L., and Schulz, K. G.: A unifying concept of coccolithophore sensitivity to changing carbonate chemistry embedded in an ecological framework, *Progress in Oceanography*, 135, 125–138, <https://doi.org/10.1016/j.pocean.2015.04.012>, 2015.
- 405



- Baumann, K.-H., Böckel, B., and Frenz, M.: Coccolith contribution to South Atlantic carbonate sedimentation, in: Coccolithophores, edited by: Thierstein, H. R. and Young, J. R., Springer Berlin Heidelberg, Berlin, Heidelberg, 367–402, https://doi.org/10.1007/978-3-662-06278-4_14, 2004.
- 410 Bown, P. R., Lees, J. A., and Young, J. R.: Calcareous nannoplankton evolution and diversity through time, in: Coccolithophores, edited by: Thierstein, H. R. and Young, J. R., Springer Berlin Heidelberg, Berlin, Heidelberg, 481–508, https://doi.org/10.1007/978-3-662-06278-4_18, 2004.
- Canadell, J. G., Le Quééré, C., Raupach, M. R., Field, C. B., Buitenhuis, E. T., Ciais, P., Conway, T. J., Gillett, N. P., Houghton, R. A., and Marland, G.: Contributions to accelerating atmospheric CO₂ growth from economic activity, carbon
415 intensity, and efficiency of natural sinks, Proc. Natl. Acad. Sci. U.S.A., 104, 18866–18870, <https://doi.org/10.1073/pnas.0702737104>, 2007.
- CoSMi Trieste: <https://cosmi.ogs.it>, 2024.
- D’Amario, B., Pérez, C., Grelaud, M., Pitta, P., Krasakopoulou, E., and Ziveri, P.: Coccolithophore community response to ocean acidification and warming in the Eastern Mediterranean Sea: results from a mesocosm experiment, Sci Rep, 10,
420 12637, <https://doi.org/10.1038/s41598-020-69519-5>, 2020.
- Daniels, C., Poulton, A., Young, J., Esposito, M., Humphreys, M., Ribas-Ribas, M., Tynan, E., and Tyrrell, T.: Species-specific calcite production reveals *Coccolithus pelagicus* as the key calcifier in the Arctic Ocean, Mar. Ecol. Prog. Ser., 555, 29–47, <https://doi.org/10.3354/meps11820>, 2016.
- Daniels, C. J., Sheward, R. M., and Poulton, A. J.: Biogeochemical implications of comparative growth rates of *Emiliana huxleyi* and *Coccolithus* species, Biogeosciences, 11, 6915–6925, <https://doi.org/10.5194/bg-11-6915-2014>, 2014.
- 425 De Bodt, C., Van Oostende, N., Harlay, J., Sabbe, K., and Chou, L.: Individual and interacting effects of CO₂ and temperature on *Emiliana huxleyi* calcification: study of the calcite production, the coccolith morphology and the coccosphere size, Biogeosciences, 7, 1401–1412, <https://doi.org/10.5194/bg-7-1401-2010>, 2010.
- Dickson, A. G., Sabine, C. L., & Christian, J. R.: Guide to best practices for ocean CO₂ measurement., North Pacific Marine
430 Science Organization, <https://doi.org/10.25607/OBP-1342>, 2007.
- Dickson, A. G. and Goyet, C.: Handbook of methods for the analysis of the various parameters of the carbon dioxide system in sea water. Version 2, <https://doi.org/10.2172/10107773>, 1994.
- Dickson, A. G. and Millero, F. J.: A comparison of the equilibrium constants for the dissociation of carbonic acid in seawater media, Deep Sea Research Part A. Oceanographic Research Papers, 34, 1733–1743, [https://doi.org/10.1016/0198-0149\(87\)90021-5](https://doi.org/10.1016/0198-0149(87)90021-5), 1987.
- 435 Diner, R. E., Benner, I., Passow, U., Komada, T., Carpenter, E. J., and Stillman, J. H.: Negative effects of ocean acidification on calcification vary within the coccolithophore genus *Calcidiscus*, Mar Biol, 162, 1287–1305, <https://doi.org/10.1007/s00227-015-2669-x>, 2015.
- Dong, S., Lei, Y., Li, T., Cao, Y., and Xu, K.: Biocalcification crisis in the continental shelf under ocean acidification,
440 Geoscience Frontiers, 14, 101622, <https://doi.org/10.1016/j.gsf.2023.101622>, 2023.



- Fiorini, S., Middelburg, J. J., and Gattuso, J.: testing the effects of elevated pCO₂ on coccolithophores (prymnesiophyceae): comparison between haploid and diploid life stages, *Journal of Phycology*, 47, 1281–1291, <https://doi.org/10.1111/j.1529-8817.2011.01080.x>, 2011.
- Gafar, N. A., Eyre, B. D., and Schulz, K. G.: A comparison of species specific sensitivities to changing light and carbonate chemistry in calcifying marine phytoplankton, *Sci Rep*, 9, 2486, <https://doi.org/10.1038/s41598-019-38661-0>, 2019a.
- 445 Gafar, N. A., Eyre, B. D., and Schulz, K. G.: Particulate inorganic to organic carbon production as a predictor for coccolithophorid sensitivity to ongoing ocean acidification, *Limnol Oceanogr Letters*, 4, 62–70, <https://doi.org/10.1002/lol2.10105>, 2019b.
- García-Romero, F., Cortés, M. Y., Rochín-Bañaga, H., Bollmann, J., Aguirre-Bahena, F., Lara-Lara, R., and Herguera, J. C.: Vertical fluxes of coccolithophores and foraminifera and their contributions to CaCO₃ flux off the coast of Ensenada, Mexico, *Cienc. Mar.*, 43, <https://doi.org/10.7773/cm.v43i4.2765>, 2017.
- 450 Gattuso, J.: Effect of calcium carbonate saturation of seawater on coral calcification, *Global and Planetary Change*, 18, 37–46, [https://doi.org/10.1016/S0921-8181\(98\)00035-6](https://doi.org/10.1016/S0921-8181(98)00035-6), 1998.
- Gazeau, F., Urrutti, P., Dousset, A., Brodu, N., Richard, M., Villeneuve, R., Pruvost, É., Comeau, S., Koechlin, H., and Pernet, F.: Toward an ecologically realistic experimental system to investigate the multigenerational effects of ocean warming and acidification on benthic invertebrates, *Limnology & Ocean Methods*, lom3.10630, <https://doi.org/10.1002/lom3.10630>, 2024.
- 455 Henderiks, J.: Coccolithophore size rules — Reconstructing ancient cell geometry and cellular calcite quota from fossil coccoliths, *Marine Micropaleontology*, 67, 143–154, <https://doi.org/10.1016/j.marmicro.2008.01.005>, 2008.
- 460 Henriksen, K., Stipp, S. L. S., Young, J. R., and Bown, P. R.: Tailoring calcite: Nanoscale AFM of coccolith biocrystals, *American Mineralogist*, 88, 2040–2044, <https://doi.org/10.2138/am-2003-11-1248>, 2003.
- Herbert, T. D., Lawrence, K. T., Tzanova, A., Peterson, L. C., Caballero-Gill, R., and Kelly, C. S.: Late Miocene global cooling and the rise of modern ecosystems, *Nature Geosci*, 9, 843–847, <https://doi.org/10.1038/ngeo2813>, 2016.
- Hoffmann, R., Kirchlechner, C., Langer, G., Wochnik, A. S., Griesshaber, E., Schmahl, W. W., and Scheu, C.: Insight into *Emiliania huxleyi* coccospheres by focused ion beam sectioning, *Biogeosciences*, 12, 825–834, <https://doi.org/10.5194/bg-12-825-2015>, 2015.
- 465 Hoppe, C. J. M., Langer, G., and Rost, B.: *Emiliania huxleyi* shows identical responses to elevated pCO₂ in TA and DIC manipulations, *Journal of Experimental Marine Biology and Ecology*, 406, 54–62, <https://doi.org/10.1016/j.jembe.2011.06.008>, 2011.
- 470 Iglesias-Rodriguez, M. D., Halloran, P. R., Rickaby, R. E. M., Hall, I. R., Colmenero-Hidalgo, E., Gittins, J. R., Green, D. R. H., Tyrrell, T., Gibbs, S. J., Von Dassow, P., Rehm, E., Armbrust, E. V., and Boessenkool, K. P.: Phytoplankton Calcification in a High-CO₂ World, *Science*, 320, 336–340, <https://doi.org/10.1126/science.1154122>, 2008.



- Intergovernmental Panel On Climate Change (Ipc): Climate Change 2021 – The Physical Science Basis: Working Group I Contribution to the Sixth Assessment Report of the Intergovernmental Panel on Climate Change, 1st ed., Cambridge University Press, <https://doi.org/10.1017/9781009157896>, 2021.
- 475 Jokiel, P. L., Rodgers, K. S., Kuffner, I. B., Andersson, A. J., Cox, E. F., and Mackenzie, F. T.: Ocean acidification and calcifying reef organisms: a mesocosm investigation, *Coral Reefs*, 27, 473–483, <https://doi.org/10.1007/s00338-008-0380-9>, 2008.
- Keul, N., Langer, G., De Nooijer, L. J., and Bijma, J.: Effect of ocean acidification on the benthic foraminifera *Ammonia* sp. is caused by a decrease in carbonate ion concentration, *Biogeosciences*, 10, 6185–6198, <https://doi.org/10.5194/bg-10-6185-2013>, 2013.
- 480 Kottmeier, D. M., Chrachri, A., Langer, G., Helliwell, K. E., Wheeler, G. L., and Brownlee, C.: Reduced H⁺ channel activity disrupts pH homeostasis and calcification in coccolithophores at low ocean pH, *Proc. Natl. Acad. Sci. U.S.A.*, 119, e2118009119, <https://doi.org/10.1073/pnas.2118009119>, 2022.
- 485 Kroeker, K. J., Kordas, R. L., Crim, R., Hendriks, I. E., Ramajo, L., Singh, G. S., Duarte, C. M., and Gattuso, J.: Impacts of ocean acidification on marine organisms: quantifying sensitivities and interaction with warming, *Global Change Biology*, 19, 1884–1896, <https://doi.org/10.1111/gcb.12179>, 2013.
- Krug, S. A., Schulz, K. G., and Riebesell, U.: Effects of changes in carbonate chemistry speciation on *Coccolithus braarudii*: a discussion of coccolithophorid sensitivities, *Biogeosciences*, 8, 771–777, <https://doi.org/10.5194/bg-8-771-2011>, 2011.
- 490 Langdon, C., Takahashi, T., Sweeney, C., Chipman, D., Goddard, J., Marubini, F., Aceves, H., Barnett, H., and Atkinson, M. J.: Effect of calcium carbonate saturation state on the calcification rate of an experimental coral reef, *Global Biogeochemical Cycles*, 14, 639–654, <https://doi.org/10.1029/1999GB001195>, 2000.
- Langer, G. and Bode, M.: CO₂ mediation of adverse effects of seawater acidification in *Calcidiscus leptoporus*, *Geochem Geophys Geosyst*, 12, 2010GC003393, <https://doi.org/10.1029/2010GC003393>, 2011.
- 495 Langer, G., Geisen, M., Baumann, K., Kläs, J., Riebesell, U., Thoms, S., and Young, J. R.: Species-specific responses of calcifying algae to changing seawater carbonate chemistry, *Geochem Geophys Geosyst*, 7, 2005GC001227, <https://doi.org/10.1029/2005GC001227>, 2006.
- Langer, G., Nehrke, G., Probert, I., Ly, J., and Ziveri, P.: Strain-specific responses of *Emiliania huxleyi* to changing seawater carbonate chemistry, *Biogeosciences*, 6, 2637–2646, <https://doi.org/10.5194/bg-6-2637-2009>, 2009.
- 500 Langer, G., Probert, I., Nehrke, G., and Ziveri, P.: The morphological response of *Emiliania huxleyi* to seawater carbonate chemistry changes: an inter-strain comparison., *J. Nanoplankton Res.*, 32, 29–36, <https://doi.org/10.58998/jnr2159>, 2011.
- Langer, G., Oetjen, K., and Brenneis, T.: On culture artefacts in coccolith morphology, *Helgol Mar Res*, 67, 359–369, <https://doi.org/10.1007/s10152-012-0328-x>, 2013.
- Langer, G., Taylor, A. R., Walker, C. E., Meyer, E. M., Ben Joseph, O., Gal, A., Harper, G. M., Probert, I., Brownlee, C., and Wheeler, G. L.: Role of silicon in the development of complex crystal shapes in coccolithophores, *New Phytologist*, 231, 1845–1857, <https://doi.org/10.1111/nph.17230>, 2021.
- 505



- Le Guevel, G., Minoletti, F., Geisen, C., Duong, G., Rojas, V., and Hermoso, M.: Multispecies expression of coccolithophore vital effects with changing CO₂ concentrations and pH in the laboratory with insights for reconstructing CO₂ levels in geological history, <https://doi.org/10.5194/egusphere-2024-1890>, 28 June 2024.
- 510 Lewis, E. R. and Wallace, D. W. R.: Program Developed for CO₂ System Calculations, <https://doi.org/10.15485/1464255>, 1998.
- McClelland, H. L. O., Barbarin, N., Beaufort, L., Hermoso, M., Ferretti, P., Greaves, M., and Rickaby, R. E. M.: Calcification response of a key phytoplankton family to millennial-scale environmental change, *Sci Rep*, 6, 34263, <https://doi.org/10.1038/srep34263>, 2016.
- 515 Mehrbach, C., Culberson, C. H., Hawley, J. E., and Pytkowicz, R. M.: Measurement of the apparent dissociation constants of carbonic acid in seawater at atmospheric pressure 1, *Limnology & Oceanography*, 18, 897–907, <https://doi.org/10.4319/lo.1973.18.6.0897>, 1973.
- Menden-Deuer, S. and Lessard, E. J.: Carbon to volume relationships for dinoflagellates, diatoms, and other protist plankton, *Limnology & Oceanography*, 45, 569–579, <https://doi.org/10.4319/lo.2000.45.3.0569>, 2000.
- 520 Menschel, E., González, H. E., and Giesecke, R.: Coastal-oceanic distribution gradient of coccolithophores and their role in the carbonate flux of the upwelling system off Concepción, Chile (36°S), *J. Plankton Res.*, 38, 798–817, <https://doi.org/10.1093/plankt/fbw037>, 2016.
- Meyer, J. and Riebesell, U.: Reviews and Syntheses: Responses of coccolithophores to ocean acidification: a meta-analysis, *Biogeosciences*, 12, 1671–1682, <https://doi.org/10.5194/bg-12-1671-2015>, 2015.
- 525 Monteiro, F. M., Bach, L. T., Brownlee, C., Bown, P., Rickaby, R. E. M., Poulton, A. J., Tyrrell, T., Beaufort, L., Dutkiewicz, S., Gibbs, S., Gutowska, M. A., Lee, R., Riebesell, U., Young, J., and Ridgwell, A.: Why marine phytoplankton calcify, *Sci. Adv.*, 2, e1501822, <https://doi.org/10.1126/sciadv.1501822>, 2016.
- Nannotax3 website: www.mikrotax.org/Nannotax3, 2024.
- Raven, J. and Crawford, K.: Environmental controls on coccolithophore calcification, *Mar. Ecol. Prog. Ser.*, 470, 137–166, <https://doi.org/10.3354/meps09993>, 2012.
- 530 Riebesell, U., Zondervan, I., Rost, B., Tortell, P. D., Zeebe, R. E., and Morel, F. M. M.: Reduced calcification of marine plankton in response to increased atmospheric CO₂, *Nature*, 407, 364–367, <https://doi.org/10.1038/35030078>, 2000.
- Ries, J. B.: A physicochemical framework for interpreting the biological calcification response to CO₂-induced ocean acidification, *Geochimica et Cosmochimica Acta*, 75, 4053–4064, <https://doi.org/10.1016/j.gca.2011.04.025>, 2011.
- 535 Rigual Hernández, A. S., Trull, T. W., Nodder, S. D., Flores, J. A., Bostock, H., Abrantes, F., Eriksen, R. S., Sierro, F. J., Davies, D. M., Ballegeer, A.-M., Fuertes, M. A., and Northcote, L. C.: Coccolithophore biodiversity controls carbonate export in the Southern Ocean, *Biogeosciences*, 17, 245–263, <https://doi.org/10.5194/bg-17-245-2020>, 2020.
- Rueden, C. T., Schindelin, J., Hiner, M. C., DeZonia, B. E., Walter, A. E., Arena, E. T., and Eliceiri, K. W.: ImageJ2: ImageJ for the next generation of scientific image data, *BMC Bioinformatics*, 18, 529, <https://doi.org/10.1186/s12859-017-1934-z>, 2017.
- 540



- Sabine, C. L., Feely, R. A., Gruber, N., Key, R. M., Lee, K., Bullister, J. L., Wanninkhof, R., Wong, C. S., Wallace, D. W. R., Tilbrook, B., Millero, F. J., Peng, T.-H., Kozyr, A., Ono, T., and Rios, A. F.: The Oceanic Sink for Anthropogenic CO₂, *Science*, 305, 367–371, <https://doi.org/10.1126/science.1097403>, 2004.
- Sheward, R. M., Poulton, A. J., Gibbs, S. J., Daniels, C. J., and Bown, P. R.: Physiology regulates the relationship between
545 coccosphere geometry and growth phase in coccolithophores, *Biogeosciences*, 14, 1493–1509, <https://doi.org/10.5194/bg-14-1493-2017>, 2017.
- Sosdian, S. M., Greenop, R., Hain, M. P., Foster, G. L., Pearson, P. N., and Lear, C. H.: Constraining the evolution of Neogene Ocean carbonate chemistry using the boron isotope pH proxy, *Earth and Planetary Science Letters*, 498, 362–376, <https://doi.org/10.1016/j.epsl.2018.06.017>, 2018.
- 550 Sun, J. and Liu, D.: Geometric models for calculating cell biovolume and surface area for phytoplankton, *J. Plankton Res.*, 25, 1331–1346, doi:10.1093/plankt/fbg096, 2003.
- Super, J. R., Thomas, E., Pagani, M., Huber, M., O’Brien, C., and Hull, P. M.: North Atlantic temperature and pCO₂ coupling in the early-middle Miocene, *Geology*, 46, 519–522, <https://doi.org/10.1130/G40228.1>, 2018.
- Šupraha, L. and Henderiks, J.: A 15-million-year-long record of phenotypic evolution in the heavily calcified
555 coccolithophore *Helicosphaera* and its biogeochemical implications, *Biogeosciences*, 17, 2955–2969, <https://doi.org/10.5194/bg-17-2955-2020>, 2020.
- Šupraha, L., Gerecht, A. C., Probert, I., and Henderiks, J.: Eco-physiological adaptation shapes the response of calcifying algae to nutrient limitation, *Sci Rep*, 5, 16499, <https://doi.org/10.1038/srep16499>, 2015.
- Walker, C. E., Taylor, A. R., Langer, G., Durak, G. M., Heath, S., Probert, I., Tyrrell, T., Brownlee, C., and Wheeler, G. L.:
560 The requirement for calcification differs between ecologically important coccolithophore species, *New Phytologist*, 220, 147–162, <https://doi.org/10.1111/nph.15272>, 2018.
- Young, J.R. Functions of Coccoliths. In: Winter, A. and Siesser, W.G., Eds., *Coccolithophores*, Cambridge University Press, New York, 13-27, 1994.
- Young, J. R. and Ziveri, P.: Calculation of coccolith volume and its use in calibration of carbonate flux estimates, 2000.
- 565 Zachos, J., Pagani, M., Sloan, L., Thomas, E., and Billups, K.: Trends, Rhythms, and Aberrations in Global Climate 65 Ma to Present, *Science*, 292, 686–693, <https://doi.org/10.1126/science.1059412>, 2001.
- Zhang, Y. G., Pagani, M., Liu, Z., Bohaty, S. M., and DeConto, R.: A 40-million-year history of atmospheric CO₂, *Phil. Trans. R. Soc. A.*, 371, 20130096, <https://doi.org/10.1098/rsta.2013.0096>, 2013.
- Ziveri, P., De Bernardi, B., Baumann, K.-H., Stoll, H. M., and Mortyn, P. G.: Sinking of coccolith carbonate and potential
570 contribution to organic carbon ballasting in the deep ocean, *Deep Sea Research Part II: Topical Studies in Oceanography*, 54, 659–675, <https://doi.org/10.1016/j.dsr2.2007.01.006>, 2007.